

# Influenza A Virus Acquires Enhanced Pathogenicity and Transmissibility after Serial Passages in Swine

Kai Wei,<sup>a</sup> Honglei Sun,<sup>a</sup> Zhenhong Sun,<sup>a</sup> Yipeng Sun,<sup>a</sup> Weili Kong,<sup>a</sup> Juan Pu,<sup>a</sup> Guangpeng Ma,<sup>b</sup> Yanbo Yin,<sup>c</sup> Hanchun Yang,<sup>a</sup> Xin Guo,<sup>a</sup> Kin-Chow Chang,<sup>d</sup> Jinhua Liu<sup>a</sup>

Key Laboratory of Animal Epidemiology and Zoonosis, Ministry of Agriculture, College of Veterinary Medicine, China Agricultural University, Beijing, China<sup>a</sup>; China Rural Technology Development Center, Beijing, China<sup>b</sup>; College of Animal Science and Veterinary Medicine, Qingdao Agricultural University, Qingdao, Shandong, China<sup>c</sup>; School of Veterinary Medicine and Science, University of Nottingham, Sutton Bonington Campus, Loughborough, United Kingdom<sup>d</sup>

## ABSTRACT

Genetic and phylogenetic analyses suggest that the pandemic H1N1/2009 virus was derived from well-established swine influenza lineages; however, there is no convincing evidence that the pandemic virus was generated from a direct precursor in pigs. Furthermore, the evolutionary dynamics of influenza virus in pigs have not been well documented. Here, we subjected a recombinant virus (rH1N1) with the same constellation makeup as the pandemic H1N1/2009 virus to nine serial passages in pigs. The severity of infection sequentially increased with each passage. Deep sequencing of viral quasiespecies from the ninth passage found five consensus amino acid mutations: PB1 A469T, PA I129T, NA N329D, NS1 N205K, and NEP T48N. Mutations in the hemagglutinin (HA) protein, however, differed greatly between the upper and lower respiratory tracts. Three representative viral clones with the five consensus mutations were selected for functional evaluation. Relative to the parental virus, the three viral clones showed enhanced replication and polymerase activity *in vitro* and enhanced replication, pathogenicity, and transmissibility in pigs, guinea pigs, and ferrets *in vivo*. Specifically, two mutants of rH1N1 (PB1 A469T and a combination of NS1 N205K and NEP T48N) were identified as determinants of transmissibility in guinea pigs. Crucially, one mutant viral clone with the five consensus mutations, which also carried D187E, K211E, and S289N mutations in its HA, additionally was able to infect ferrets by airborne transmission as effectively as the pandemic virus. Our findings demonstrate that influenza virus can acquire viral characteristics that are similar to those of the pandemic virus after limited serial passages in pigs.

## IMPORTANCE

We demonstrate here that an engineered reassortant swine influenza virus, with the same gene constellation pattern as the pandemic H1N1/2009 virus and subjected to only nine serial passages in pigs, acquired greatly enhanced virulence and transmissibility. In particular, one representative pathogenic passaged virus clone, which carried three mutations in the HA gene and five consensus mutations in PB1, PA, NA, NS1, and NEP genes, additionally was able to confer respiratory droplet transmission as effectively as the pandemic H1N1/2009 virus. Our findings suggest that pigs can readily induce adaptive mutational changes to a precursor pandemic-like virus to transform it into a highly virulent and infectious form akin to that of the pandemic H1N1/2009 virus, which underlines the potential direct role of pigs in promoting influenza A virus pathogenicity and transmissibility.

In March and early April 2009, a novel H1N1 influenza A virus (IAV) emerged in Mexico and the United States and rapidly triggered the first human pandemic of the 21st century (1). Phylogenetic and genetic studies revealed that the eight-gene segments of the H1N1/2009 virus were generated through reassortment between well-established swine influenza lineages, the Eurasian avian-like lineage, and the North American triple-reassortant lineage (1–3). Furthermore, structural and serological studies of its hemagglutinin (HA) have demonstrated that the H1N1/2009 virus is antigenically similar to 1918-like and classical swine H1N1 viruses (4, 5). Phylogenetically, the H1N1/2009 virus corresponds to a genetic ancestry of swine viruses, suggesting either an increased evolutionary rate or a long but unnoticed period of circulation in pigs prior to its 2009 pandemic emergence. Bayesian molecular clock analysis demonstrated that the evolutionary rate preceding the H1N1/2009 virus pandemic was typical for swine influenza (2). Thus, the reassortment of Eurasian avian-like and North American triple-reassortant swine lineages may not have occurred just before the 2009 pandemic; instead, a single reassortant (pandemic H1N1-like) virus may have been crypti-

cally circulating in an unidentified host species for years before the outbreak in humans (2, 3). However, the reassortment dynamics of H1N1/2009 virus have not been determined in swine or humans by epidemiological surveillance (2, 6).

In our earlier study, we constructed a reassortant swine H1N1 influenza virus (rH1N1) with the same phylogenetic gene combination as the pandemic H1N1/2009 virus. The neuraminidase (NA) and matrix (M) gene segments were from

Received 10 June 2014 Accepted 1 August 2014

Published ahead of print 6 August 2014

Editor: D. S. Lyles

Address correspondence to Jinhua Liu, ljh@cau.edu.cn.

K.W. and H.S. contributed equally to this work.

Supplemental material for this article may be found at <http://dx.doi.org/10.1128/JVI.01679-14>.

Copyright © 2014, American Society for Microbiology. All Rights Reserved.

doi:10.1128/JVI.01679-14

a Eurasian avian-like H1N1 swine influenza virus, and the other six genes were from a triple-reassortant H1N2 swine influenza virus (7). Unlike the pandemic H1N1/2009 virus, we found that this H1N1/2009-like virus is not able to confer virus transmissibility in guinea pigs, and that additional amino acid mutations are needed to make the virus as transmissible as the pandemic IAV (7). Consequently, the question remains: can IAVs acquire the characteristics of H1N1/2009 virus, including specific amino acid mutations of the H1N1/2009 virus, after undergoing adaptive changes in a specific host?

Thus far, adaptive changes of IAVs have been studied mainly by serial viral passages in laboratory species (8, 9). Mice have been used extensively for investigating pathogenic mechanisms and host range determinants (10, 11). Guinea pigs and ferrets support IAV transmission and have been used as models for IAV adaptation studies (12–16). Pigs, on the other hand, can be naturally or experimentally infected with IAVs. They can serve as mixing vessels or intermediate hosts for the generation of novel reassortant viruses (17, 18). Therefore, pigs most likely perform key roles in the evolutionary process of influenza viruses and in their cross-species transmission (19, 20). The emergence of the H1N1/2009 virus provides further evidence of the role of pigs in the influenza virus ecosystem. However, there is no direct supporting evidence to show that the pandemic H1N1/2009 virus was derived from pigs. Thus, it is important to investigate the adaptive evolution of IAVs in pigs.

To explore the evolutionary genesis of the pandemic H1N1/2009 virus, we performed serial passages of the rH1N1 construct in pigs and examined its sequential replication, pathogenicity, and transmissibility. By the ninth passage, the resulting viral population with five consensus mutations had acquired marked pathogenicity and in-contact transmissibility in swine and guinea pigs. Moreover, one particular representative viral clone, with three additional HA mutations, also acquired the ability for efficient airborne transmission between ferrets.

## MATERIALS AND METHODS

**Ethics statement.** All animal research was approved by the Beijing Association for Science and Technology (approval identifier [ID] SYXK [Beijing] 2007-0023) and performed in compliance with the Beijing Laboratory Animal Welfare and Ethics guidelines, as issued by the Beijing Administration Committee of Laboratory Animals, and in accordance with the China Agricultural University (CAU) Institutional Animal Care and Use Committee guidelines (ID SKLAB-B-2010-003) approved by the Animal Welfare Committee of CAU.

**Viruses and cells.** The parental rH1N1 virus was described previously and was generated by reverse genetics (7), in which the NA and M genes from A/Swine/Fujian/204/2007 (accession numbers [FJ536810](#) to [FJ536817](#)) and the other six genes from A/Swine/Guangdong/1222/2006 (accession numbers [GU086078](#) to [GU086085](#)) were from the same phylogenetic cluster of H1N1/2009 viruses. The pandemic H1N1/2009 virus, A/Swine/Shandong/731/2009 (SD731), was isolated from swine in Shandong Province, China, in December 2009. Its complete genomic sequence is available in GenBank (accession numbers [JF951848](#) to [JF951855](#)). Viruses were titrated in MDCK cells to determine the median tissue culture infectious dose (TCID<sub>50</sub>) by the Reed and Muench method (21). MDCK cells and A549 human lung adenocarcinoma cells were maintained in Dulbecco's modified Eagle's medium (DMEM; Gibco) containing 10% fetal bovine serum (FBS; Gibco) and 1% antibiotics (Invitrogen). *In vivo* and *in vitro* experiments involving rH1N1 and H1N1/2009 viruses were conducted in biosafety level (BSL) 2+ containment, as approved by the

Ministry of Agriculture of China and the China National Accreditation Service for Conformity Assessment.

**Serial passages, clinical measurements, and sampling.** Landrace hybrid pigs, aged 4 to 5 weeks at the outset, were sourced from a high-health-status herd (porcine reproductive and respiratory syndrome [PRRS] virus free) and were IAV and antibody (H1, H3, H5, H7, and H9) negative by M gene PCR and hemagglutination inhibition assays prior to the start of the study. Passaging was established initially in one pig by intranasal inoculation with a total dose of 10<sup>6</sup> TCID<sub>50</sub> rH1N1 virus, delivered in a final volume of 2.5 ml per nostril, using a mucosal atomization device (MAD; Wolfe Tory Medical, Inc.) to mimic aerogenic infection. The animal was euthanized at 4 days postinoculation (dpi). The lung was removed whole and lavaged with 200 ml phosphate-buffered saline (PBS) to obtain bronchoalveolar lavage fluid (BALF), and the nasal wash was performed with 10 ml PBS (containing 1% antibiotics). Five ml BALF and two ml nasal wash were combined to infect the next pig. The remaining nasal wash, BALF, and the collected tissue samples of each passage were stored at –80°C. During each passage, veterinary assessment was made at two fixed time points daily. Clinical parameters determined were rectal temperature, appetite, mental changes, bilateral nasal and ocular discharges, wheezing, and coughing.

**Gross and microscopic examination of lung lesions.** During necropsy, a mean value of the percentage of gross lesions (defined as dark red consolidation) was calculated for the pulmonary lobes. The lung tissue was collected and fixed in 10% phosphate-buffered formalin for histopathological examination, which was performed as described previously (22). Tissue sections of lungs were stained with hematoxylin and eosin (H&E) and examined microscopically for bronchiolar epithelial changes and peribronchiolar inflammation. Lesion severity was scored by the distribution or by the extent of lesions within the sections examined (22) with the following scale: 0, no visible changes; 1+, mild focal or multifocal change; 2+, moderate multifocal change; 3+, moderate diffuse change; 4+, severe diffuse change. Two independent pathologists scored all slides from blinded experimental groups.

**Deep sequencing.** Viral RNA was extracted from nasal wash and BALF of the pigs after nine serial passages with the parental rH1N1 virus using the High Pure RNA isolation kit (Roche). RNA was subjected to reverse transcription-PCR (RT-PCR) using 18 primer sets that cover the entire viral genome. These primer sets were designed according to the genome sequences of the rH1N1 virus and by using Primer Premier 5.0 software. The fragments, approximately 600 to 800 nucleotides in length, were sequenced using the Illumina HiSeq2000 sequencing platform in the Chinese National Human Genome Center, Shanghai. Briefly, a library was constructed with TruSeq DNA sample prep kit set A. The DNA library was diluted and hybridized to the paired-end sequencing flow cells. DNA clusters were generated on a cBot cluster generation system with the TruSeq PE cluster generation kit v2, followed by sequencing on a HiSeq 2000 system with the TruSeq SBS kit v2. The threshold for the detection of single-nucleotide polymorphisms (SNP) was set manually at 10% of the population.

**Sanger sequencing.** Genome RNAs of viral clones were extracted from culture supernatants using the QIAamp viral RNA kit (Qiagen). Genes were reverse transcribed and amplified using a OneStep RT-PCR kit (Qiagen). Primers were the same as those used in the deep sequencing assay. The amplified cDNA products were excised from agarose gels and purified using a QIAquick gel extraction kit (Qiagen). Full-genome DNAs were Sanger sequenced by Huada Zhongsheng Scientific Corporation, and the sequence data were analyzed using GenScan software.

**Viral growth kinetics.** Confluent MDCK or A549 cells were infected with L2, N9, L18, or parental rH1N1 virus at a multiplicity of infection (MOI) of 0.001 in serum-free DMEM containing 2 mg/ml tolylsulfonyl phenylalanyl chloromethyl ketone (TPCK)-trypsin (Sigma-Aldrich) and were cultured in a 37°C CO<sub>2</sub> incubator. Cell supernatants were harvested every 12 h until 72 h postinoculation (hpi) and titrated by the TCID<sub>50</sub> method on MDCK cells.

**Western blotting.** MDCK cells infected with L2, N9, L18, or parental rH1N1 virus were collected at 12 or 24 hpi. The protein samples derived from cell lysates were heated at 100°C for 5 min and then separated on a 10% sodium dodecyl sulfate-polyacrylamide gel and transferred to a polyvinylidene difluoride (PVDF) membrane (Bio-Rad). Membranes were incubated with mouse anti-NP monoclonal antibody (Abcam) and horseradish peroxidase (HRP)-conjugated rabbit anti-goat IgG (GE Healthcare, Inc.). The membranes were developed with an enhanced chemiluminescence kit (Pierce).

**Polymerase activity assay.** A combination of wild-type or mutant PB2, PB1, PA, and NP expression plasmids (125 ng each) was cotransfected into 293T cells with the luciferase reporter plasmid pYH-Luci (10 ng) and internal control plasmid renilla (5 ng). At 24 h posttransfection, a luciferase assay was performed using the Dual-Luciferase reporter assay system (Promega) and read using a GloMax 96 microplate luminometer (Promega).

**Generation of mutant viruses by reverse genetics.** RT-PCR-derived mutant viral genes were cloned into a dual-promoter plasmid, pHW2000. MDCK and 293T cells (1:2 mixture) were cocultured in 6-well plates and transfected with 0.5 µg of each of the eight plasmids and 10 µl Lipofectamine 2000 (Invitrogen) in a total volume of 1 ml of Opti-MEM (Invitrogen) into each well. After incubation at 37°C for 6 h, the transfection mixture was removed from the cells and 2 ml of Opti-MEM containing 1 mg/ml of TPCK-trypsin was added. After 48 h, the supernatant was used to inoculate MDCK cells (cultured in a T75 flask) to produce stock virus. Viral RNA was extracted and analyzed by RT-PCR, and each viral segment was sequenced to confirm the identity of the virus. Stock viruses were titrated by the TCID<sub>50</sub> method on MDCK cells.

**Infection and transmission in pigs.** Twelve Landrace hybrid pigs, aged 4 to 5 weeks, were randomly assigned into four separate groups of three. All pigs were sourced from a high-health-status herd (PRRS virus free and IAV and antibody negative). Each pig was infected intranasally with a total dose of 10<sup>6</sup> TCID<sub>50</sub> test virus delivered in a final volume of 2.5 ml per nostril. Three naive animals were introduced into each cage 24 h later. Beginning at 1 dpi, nasal swabs were collected daily and titrated on MDCK cells. The clinical symptoms of each pig were recorded daily. The directly infected pigs were euthanized at 6 dpi, and the contact pigs were euthanized at 7 days postcontact (dpc). Lungs were removed for viral load assessment and histopathology.

**Contact transmission in guinea pigs.** Female Hartley strain SPF/VAF guinea pigs (serologically negative for IAVs) that weighed between 300 and 350 g were obtained from Vital River Laboratories. They were anesthetized by intramuscular injection of Zoletil 100 (tiletamine-zolazepam; 10 to 15 mg/kg of body weight; Virbac) prior to all handling procedures, including inoculation, nasal washes, and collection of blood. Three guinea pigs each were intranasally inoculated with a dose of 10<sup>6</sup> TCID<sub>50</sub> of a specific virus in 200 µl PBS. Each inoculated animal was placed in a new cage with one naive guinea pig at 1 dpi. Nasal washes were collected from all six guinea pigs at 2, 4, 6, 8, and 10 dpi. The ambient conditions for this study were set at 20 to 25°C and 30% to 40% relative humidity.

**Respiratory droplet transmission in ferrets.** Six- to twelve-month-old male Angora ferrets (Angora Ltd.), serologically negative by the hemagglutination inhibition assay for currently circulating influenza viruses (H1, H3, H5, H7, and H9), were used. At the start of the experiment, all ferrets were greater than 1.0 kg (range, 1.12 to 1.58 kg) in weight. Ferrets that lost more than 25% of their body weight or exhibited neurological dysfunction were euthanized and submitted to postmortem examination. Baseline rectal temperature and weight measurements were obtained prior to infection. Groups of three ferrets were intranasally inoculated with 10<sup>6</sup> TCID<sub>50</sub> of test virus and housed in specially designed cages inside an isolator. At 1 dpi, three naive animals were placed in an adjacent cage (5 cm away), separated by a double-layered net divider that allowed free passage of air. Nasal washes were collected at 2-day intervals beginning at 2 dpi (1 day postexposure [dpe]) and were titrated in MDCK cells. Directly infected and exposed ferrets were euthanized at 8 dpi and 9 dpe,

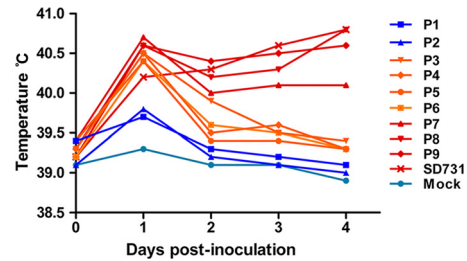


**FIG 1** Passing of rH1N1 virus in pigs caused progressive body temperature rise. Rectal temperature was taken at two fixed time points daily from 0 to 4 dpi for P1 and P2 (blue), P3 to P6 (orange), P7 to P9, positive-control SD731 virus-inoculated (red), and mock-infected (cyan) pigs. All values shown represent the mean rectal temperature per day for each animal. A temperature higher than 39.5°C is considered pyrexia in pigs.

respectively. The ambient conditions for these studies were set at 20 to 25°C and 30% to 40% relative humidity. The horizontal airflow in the isolator was at 0.1 m/s and was directed from the inoculated to exposed animals.

**Statistical analyses.** Statistically significant differences between experimental groups were determined using the analysis of variance (ANOVA) method. A *P* value of <0.05 was considered statistically significant.

## RESULTS

**rH1N1 virus showed enhanced pathogenicity after nine passages in pigs.** To study the natural evolution of a virus that has the same gene combination as the pandemic H1N1/2009 virus, we passaged the rH1N1 virus (7) in pigs by one-on-one delivery. Passaging began with the nasal inoculation of 10<sup>6</sup> TCID<sub>50</sub> of the rH1N1 virus. Clinical signs were monitored daily until 4 dpi, at which time the animal was euthanized to collect nasal wash and BALF. The mixture of the nasal wash (2 ml) and BALF (5 ml) subsequently was used to inoculate the next pig intranasally (passage 2 [P2]). This procedure was repeated until P9.

Overall, the clinical signs elicited from P1 to P9 virus-infected pigs increased steadily from mild to severe. The P1 and P2 virus-infected pigs did not show any overt clinical signs from 1 to 4 dpi, although a small transient elevation in body temperature was observed at 1 dpi (Fig. 1). The P3 to P6 virus-infected pigs developed pyrexia (>40.0°C) only at 1 dpi (Fig. 1). Strikingly, the P7 to P9 virus-infected pigs showed sustained pyrexia (Fig. 1) accompanied by clear symptoms of depression, anorexia, tremors, and nasal and ocular discharge. The P8 virus-infected pigs displayed severe and earlier onset of clinical signs with noticeable wheezing and coughing at 4 dpi. The P9 virus-infected pigs were the most severely affected, with the earliest onset of clinical symptoms. Three control pigs inoculated with SD731 virus (a virulent H1N1/2009 virus) at 10<sup>6</sup> TCID<sub>50</sub> developed clinical signs (pyrexia, wheezing, and coughing) from 2 to 4 dpi that were similar to those observed in the P9 virus-infected pigs.

To examine the pathological effects of multiply passaged rH1N1 viruses, lungs from infected pigs were examined postmortem. Gross lesions of P1 to P9 virus-infected lungs showed increasing severity (Fig. 2). P1 and P2 virus-infected lungs appeared normal, but P3 to P8 virus-infected lungs showed increasing multifocal areas of consolidation in the cardiac, diaphragmatic, and intermediate lobes. P6 virus-infected lung displayed extensive hyperemia, edema, and diffuse consolidation over the entire lung (Fig. 2). P9 virus-infected lung had the most severe lesions with



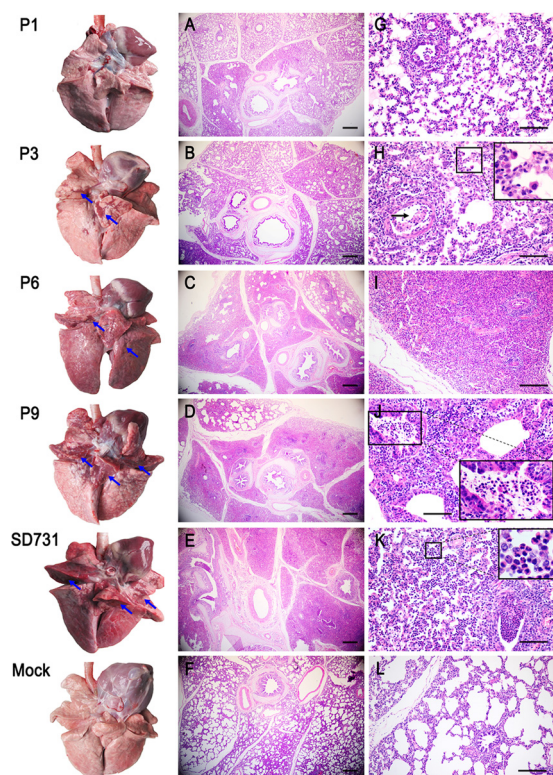


**FIG 2** Passing of rH1N1 virus in pigs led to increasing pulmonary damage. Gross and histopathological examinations were performed on the respiratory tracts of infected pigs at 4 dpi. Representative gross (left) and corresponding histological (H&E staining) findings at low (middle) and high (right) magnification are presented. (A and G) P1 virus-infected lung showed mild bronchopneumonia with minor lymphocytic infiltration. (B and H) P3 virus-infected lung had moderate bronchopneumonia with inflammatory cell infiltrates in the alveoli and interstitium (boxed area magnified) and loss of epithelial lining (black arrow in H). (C and I) P6 virus-infected lung showed severe bronchopneumonia with hemorrhage, edema, and diffuse consolidation. (D and J) P9 virus-infected lung displayed extensive consolidation in all lobes and severe bronchopneumonia with diffuse infiltration of neutrophils and alveolar macrophages (the boxed area is magnified). (E and K) Virulent SD731 virus-infected lung showed severe bronchopneumonia similar to the changes found in the P9 lung. (F and L) Mock-infected lung showed normal morphology. Blue arrows (left) indicate pulmonary tissue consolidation. Results shown are typical of three independent examinations for each animal. Scale bar, 200  $\mu$ m.

extensive consolidation in all lobes, which resembled the lung pathology found in SD731 virus-infected pigs (Fig. 2). Microscopic lesions from P1 to P9 virus-infected lungs increased from mild bronchitis to severe peribronchiolitis and bronchopneumonia, which were characterized by edema and diffuse infiltration of inflammatory cells in the alveolar lumen and bronchioles (Fig. 2). The histopathology score of the P9 virus-infected lung was up to 3.5, and those of P6, P3, and P1 virus-infected pigs were up to 3.0, 2.0, and 1.0, respectively (Fig. 3). Together, these findings showed that the passing of rH1N1 virus in swine progressively enhanced its pathogenicity.

To evaluate the ability of each passaged rH1N1 virus to replicate in the pig, we ascertained virus titers of nasal washes, BALF, and lung tissue at 4 dpi. Titers progressively increased with each passage; at P9, virus titers were as high as those derived from SD731 virus-inoculated pigs ( $P > 0.05$ ) (Fig. 4). On the basis of

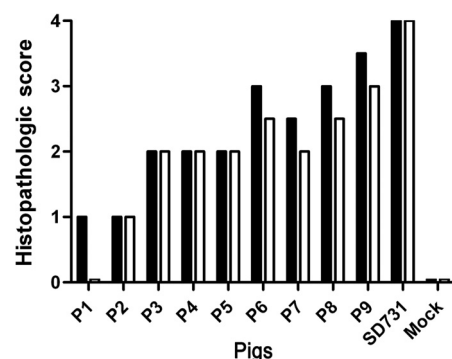


**FIG 3** Histopathological lung lesion scores from progressively passaged rH1N1 virus-infected pigs at 4 dpi. Microscopic lesions of the cardiac lobes (black bars) and diaphragmatic lobes (white bars) were evaluated and assigned a score of 0 to 4 based on evaluation criteria described in Materials and Methods. All values shown represent the mean score from three independent evaluations of each lung. A representative score from SD731 virus-infected lungs served as a positive control.

clinical signs and pathological changes, we concluded that the rH1N1 virus had acquired an SD731 virus-like pathogenic phenotype after nine passages in swine.

**Selection of three representative viral clones from P9 quasi-species.** The passing of IAVs in animals would result in the natural selection of heterogeneous mixtures of viruses with various mutations, the so-called viral quasispecies (23, 24). To assess possible genetic diversity of viral quasispecies in the upper and lower respiratory tract of the P9 virus-infected pigs, we performed deep sequencing on viral RNA derived from nasal wash and BALF. Five consensus mutations were found in the virion populations of both the nasal wash and BALF compartments (frequencies of  $>91\%$ ): PB1 A469T, PA I129T, NA N329D, NS1 N205K, and NEP T48N (Table 1). Mutations detected in HA showed apparent divergence between the nasal wash and BALF; D187E, K211E, and S289N mutations were frequent in the BALF, whereas M227I, S271P, and I295V mutations were frequent in the nasal wash (Table 1). This HA finding indicates that the genetic composition of viral quasispecies in the upper and lower respiratory tract of the P9 virus-infected pigs was distinctly different. Moreover, within each compartment, the mutational frequencies of the HA protein ranged from 26.46% to 55.89% in BALF and 54.72% to 66.35% in nasal wash (Table 1), indicating relatively low mutational consensus in viral populations within each location of the airway.

To select representative P9 viral clones from the viral quasispecies, we performed plaque purification and genome sequencing to establish the sequence composition of individual clones. We isolated randomly 20 lung viral clones (L1 to L20) and 20 nasal viral clones (N1 to N20) originating from the BALF and nasal wash, respectively, of the P9 virus-infected pigs. Four of the five consensus mutations (PB1 A469T, NA N329D, NS1 N205K, and NEP T48N) were identified in all 40 clones, and PA I129T was identified in 36/40 clones. In contrast, the HA protein showed much mutational variability (see Table S1 in the supplemental material). Among all HA mutations in the 20 lung viral clones, D187E, K211E, and S289N mutations accounted for twelve, five, and seven mutations, respectively. Most P9 viruses with the D187E mutation also had the K211E and/or S289N mutation. Con-

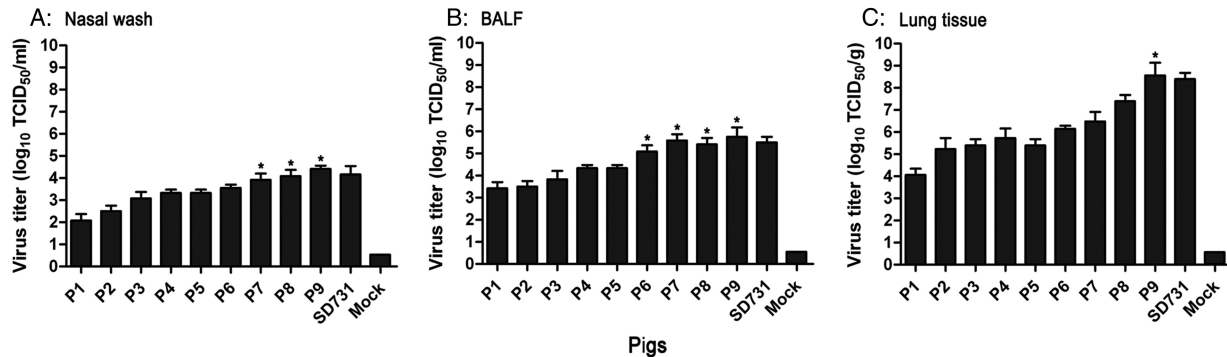


**FIG 4** Viral titers in nasal washes, BALFs, and lungs of progressively passed rH1N1 virus-infected pigs at 4 dpi. Viral titers of nasal washes (A) and BALF (B) were directly determined by TCID<sub>50</sub> assays on MDCK cells. (C) Collected lung tissues were weighed, and 10% (vol/vol) homogenates were prepared in cold PBS. Virus titers in cleared homogenates were determined by TCID<sub>50</sub> assays on MDCK cells. All values shown are means  $\pm$  standard deviations (SD) from three independent experiments for each sample. Representative SD731 virus titers derived from corresponding sites of infected pigs served as positive controls. An asterisk indicates that the virus titer was not significantly different from that of the SD731 virus group ( $P > 0.05$  by ANOVA). The virus detection limit was 10 TCID<sub>50</sub>.

versely, in the 20 nasal viral clones, mutations M227I, S271P, and I295V in the HA protein were most frequent, occurring in combinations of two (5 clones) or three (10 clones) mutations (see Table S1).

We next selected three representative viral clones harboring all five of the consensus mutations (PB1 A469T, PA I129T, NA N329D, NS1 N205K, and NEP T48N) in combination with the D187E, K211E, and S289N mutations (as a representative lower respiratory tract virus, named L2), with the M227I, S271P, and I295V mutations (as a representative upper respiratory tract virus, named N9), or with no mutational change in the HA (named L18).

**Representative P9 virus-derived viral clones exhibited enhanced replication *in vitro*.** To evaluate the replicative abilities of the L2, N9, and L18 viral clones, they were used to infect MDCK cells and human A549 cells at an MOI of 0.001 to determine virus titers over 72 hpi. For MDCK cells, the titers of the L2, N9, and L18 viruses were higher than those of the parental rH1N1 virus at the

initial 12 to 48 hpi, with significant differences at 12 to 24 hpi ( $P < 0.05$ ) (Fig. 5A). We also assessed the levels of viral nucleoprotein (NP) in MDCK cells at 12 and 24 hpi. Protein expression of NP by the three P9 viruses was higher than that of the rH1N1 virus (Fig. 5B). Furthermore, with A549 cells, the titers of the L2, N9, and L18 viruses were significantly higher than those of rH1N1 virus at almost all time points ( $P < 0.05$ ) (Fig. 5C). These results clearly demonstrated that the replication of the three P9 viruses *in vitro* was significantly greater than that of the parental rH1N1 virus.

**PB1 A469T mutation conferred enhanced polymerase activity to parental rH1N1 RNP complex.** Since there is close correlation between the activity of the viral ribonucleoprotein (RNP) complex and viral adaptation, replication, and pathogenicity (10, 25), the functional effect of PB1 A469T and PA I129T consensus mutations on viral polymerase activity was assessed. The polymerase activity of the parental rH1N1 RNP complex was determined by luciferase assay through cotransfection into 293T cells of expression plasmids encoding PB2, PB1, PA, and NP, along with

**TABLE 1** Mutation analysis of viral quasispecies in BALF and nasal wash of P9 virus-infected pigs

Protein	Nucleotide		Frequency <sup>a</sup> (%) in:		Position		Amino acid	
	Reference	Mutation	BALF	Nasal wash	Nucleotide	Amino acid	Reference	Substitution <sup>c</sup>
PB2	A	G	50.13	43.12	1185	386	V	—
PB1	G	A	96.62	95.44	1429	469	A	T
PB1	G	A	92.50	93.68	204	60	E	—
PA	T	C	95.41	93.15	412	129	I	T
HA	C	A	55.89	ND	644	187	D	E
HA	A	G	26.46	ND	716	211	K	E
HA	G	A	40.23	ND	949	289	S	N
HA	G	A	ND <sup>b</sup>	66.35	764	227	M	I
HA	T	C	ND	54.72	894	271	S	P
HA	A	G	ND	62.23	966	295	I	V
NP	G	A	27.70	32.46	1413	456	L	—
NA	A	G	91.47	93.67	1005	329	N	D
M2	G	A	92.06	95.34	313	96	L	—
NS1	C	A	97.45	96.18	641	205	N	K
NEP	C	A	98.41	97.35	641	48	T	N

<sup>a</sup> All mutations shown have a frequency of  $>10\%$ .

<sup>b</sup> ND, not detected.

<sup>c</sup> —, silent substitution.

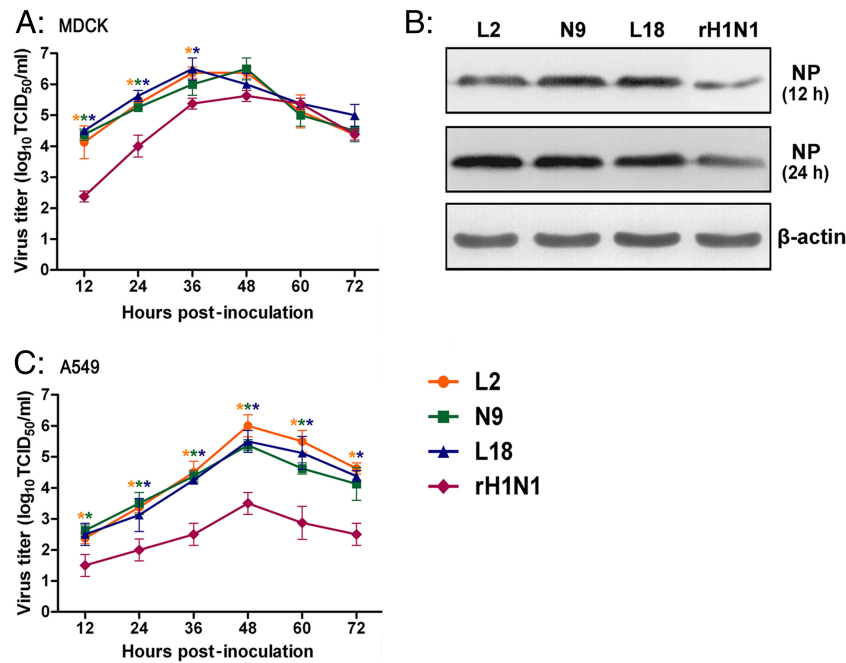


FIG 5 Three representative P9 viral clones exhibited enhanced replication in MDCK and A549 cells. Viable virus output from MDCK (A) or A549 (C) cells infected with three viruses derived from the P9 infection (L2, N9, and L18) and parental rH1N1 viruses, at an MOI of 0.001, was determined by TCID<sub>50</sub> assay at 12, 24, 36, 48, 60, and 72 hpi. The values are expressed as means  $\pm$  SD ( $n = 3$ ). An asterisk indicates that the value of the corresponding virus was significantly different from that of the rH1N1 virus ( $P < 0.05$  by ANOVA). (B) Western blots for viral NP detection in MDCK cells at 12 and 24 hpi;  $\beta$ -actin was used as a loading control. The Western blot results are representative of three independent experiments.

luciferase reporter pYH-Luci plasmid and an internal renilla control plasmid (Fig. 6). The replacement of parental PA with PA I129T plasmid had little effect on RNP activity. However, replacement of parental PB1 with PB1 A469T plasmid resulted in about a 6-fold increase in polymerase activity ( $P < 0.05$ ) (Fig. 6). This

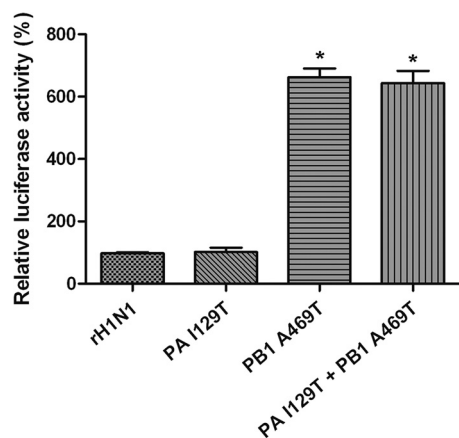


FIG 6 Activity of parental rH1N1 RNP complex reconstituted with P9 virus-derived PA I129T and PB1 A469T mutants. A combination of four plasmids expressing RNP components of parental rH1N1 virus (PB2, PB1, PA, and NP), luciferase reporter plasmid pYH-Luci, and an internal renilla control plasmid were transfected into 293T cells. Mutant PA I129T or PB1 A469T plasmid was substituted for the corresponding wild-type rH1N1 plasmids as indicated. Values shown represent means  $\pm$  SD for three independent experiments, normalized to the activity of parental rH1N1 RNP complex (100%). \*,  $P < 0.05$  compared to the correspondingly transfected rH1N1 response.

result indicates that PB1 A469T is an important contributor to the enhanced replicative ability of P9 viruses.

**Representative P9-derived viruses exhibited enhanced pathogenicity and transmissibility in swine.** To assess the pathogenicity of the three representative P9 virus-derived viral clones (L2, N9, and L18 viruses) in relation to parental rH1N1 virus *in vivo*, each group of three pigs was infected intranasally with each virus at  $10^6$  TCID<sub>50</sub>. At 1 dpi, three naive in-contact pigs were added to each infected group. All pigs directly infected with L2, N9, and L18 viruses showed typical flu-like symptoms (i.e., pyrexia, depression, nasal discharge, wheezing, and coughing) associated with moderate to severe lung lesions, and most in-contact pigs in these three groups also displayed mild pyrexia, nasal discharge, and similar pathological damage (Table 2 and Fig. 7). In contrast, the rH1N1-inoculated and in-contact pigs showed no obvious clinical symptoms and pulmonary damage (Table 2 and Fig. 7). Pathological lung scores were  $2.8 \pm 0.1$ ,  $2.5 \pm 0.1$ , and  $2.3 \pm 0.3$  in the L2, N9, and L18 directly infected groups, respectively, which were significantly higher than the scores of the rH1N1 inoculated pigs ( $0.3 \pm 0.1$ ;  $P < 0.05$ ).

Virus shedding or presence was monitored from nasal swabs of directly infected pigs from 1 to 6 dpi and of in-contact pigs from 1 to 7 dpc. Viral shedding was detected in all pigs directly infected with L2, N9, L18, and rH1N1 viruses at 1 to 6 dpi. Peak titers of the three P9 viruses were approximately 10-fold higher than those of the rH1N1 virus (Fig. 8). Notably, all L2, N9, and L18 in-contact pigs shed virus, but no virus was detected in rH1N1 in-contact pigs throughout the screening period (Fig. 8). Together, these data indicate that the pathogenicity and transmissibility of P9 virus-



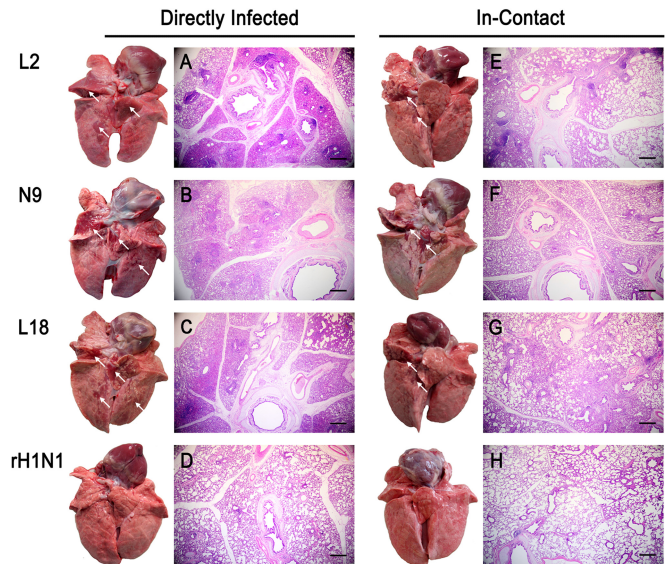


FIG 7 Gross pathology and histopathology of lungs from pigs infected with three representative P9-derived viruses. Lungs were isolated from pigs directly infected with the L2, N9, L18, and control parental rH1N1 viruses at 6 dpi or as in-contacts at 8 dpi (7 dpc). (A to C) Lungs from directly infected L2, N9, and L18 viruses showed moderate pulmonary consolidation (white arrows) and moderate to severe bronchopneumonia with interstitial pulmonary edema and inflammatory cell infiltrates in alveolar space. (E to G) Lungs from in-contact pigs exposed to L2, N9, and L18 viruses also showed mild lung consolidation (white arrows) and mild to moderate bronchopneumonia. (D and H) There was no apparent pathological damage detected in lungs of rH1N1-infected and in-contact pigs. Images shown are representative of three pigs from three independent experiments. Scale bar, 200  $\mu$ m.

derived L2, N9, and L18 viruses were much greater than that of the parental rH1N1 virus.

**Representative P9 virus-derived viruses also acquired in-contact transmissibility in guinea pigs.** Our previous study demonstrated that the parental rH1N1 virus is not transmissible between guinea pigs, unlike the pandemic H1N1/2009 virus, which transmits efficiently in these animals (7). To determine whether the passaged virus had acquired this transmissibility, guinea pigs were infected with the P9 virus-derived L2, N9, L18, or parental rH1N1 virus. Consistent with previous findings (7), there was no virus shedding from in-contact guinea pigs in the rH1N1 group (Fig. 9D). However, two of three guinea pigs in contact with guinea pigs directly infected with L2, N9, and L18 viruses developed virus shedding (Fig. 9A to C), which suggests that these viruses have largely acquired the ability to transmit infection to in-contact guinea pigs.

**Mutation PB1 A469T, and single-site combined mutations NS1 N205K and NEP T48N, in rH1N1 virus conferred in-contact transmissibility in guinea pigs.** Among the three transmissible P9 virus-derived clones, L18 virus contains the five consensus amino acid mutations with no change in HA in relation to the parental rH1N1 virus. To further determine which amino acid mutation contributes to the contact transmissibility of P9-derived viruses, we performed reverse genetics to construct four single-site mutant viruses from rH1N1, named PB1 A469T, PA I129T, NA N329D, and NS1 N205K-NEP T48N (derived from a one-nucleotide change), and two double-site mutant viruses (named PB1 A469T-PA I129T and NA N329D-NS1 N205K-NEP T48N).

TABLE 2 Clinical symptoms, pathological changes, and virus detection in pigs

Infection characteristics in:											
Directly infected pigs						In-contact pigs					
Virus	Pyrexia <sup>a</sup> (no. positive/ total no.)	Nasal discharge (no. positive/ total no.)	Wheezing/ coughing (no. positive/ total no.)	Pulmonary consolidation <sup>b</sup> (no. positive/ total no.) (%)	Microscopic lung lesion score <sup>c</sup>	Virus detection in lung <sup>d</sup> (no. positive/total no.) (titer)	Pyrexia <sup>a</sup> (no. positive/total no.)	Nasal discharge (no. positive/ total no.)	Pulmonary consolidation <sup>b</sup> (no. positive/ total no.) (%)	Microscopic lung lesion score <sup>c</sup>	Virus detection in lung <sup>d</sup> (no. positive/total no.) (titer)
L2	3/3 (40.4 $\pm$ 0.2)	3/3	3/3	3/3 (23.2 $\pm$ 3.1)	2.8 $\pm$ 0.1	3/3 (3.7 $\pm$ 0.3)	3/3 (40.1 $\pm$ 0.2)	3/3	3/3 (6.3 $\pm$ 1.6)	1.5 $\pm$ 0.2	3/3 (2.2 $\pm$ 0.4)
N9	3/3 (40.3 $\pm$ 0.2)	3/3	2/3	3/3 (19.6 $\pm$ 4.6)	2.5 $\pm$ 0.1	3/3 (3.2 $\pm$ 0.4)	3/3 (40.0 $\pm$ 0.2)	3/3	3/3 (5.1 $\pm$ 2.8)	1.7 $\pm$ 0.2	3/3 (2.1 $\pm$ 0.2)
L18	3/3 (40.3 $\pm$ 0.1)	3/3	2/3	3/3 (22.3 $\pm$ 3.2)	2.3 $\pm$ 0.3	3/3 (3.0 $\pm$ 0.1)	3/3 (40.1 $\pm$ 0.1)	3/3	3/3 (5.8 $\pm$ 2.3)	1.1 $\pm$ 0.1	3/3 (2.8 $\pm$ 0.2)
rH1N1	1/3 (39.6 $\pm$ 0.2)	3/3	0/3	1/3 (<1)	0.3 $\pm$ 0.1	0/3 (<1) <sup>e</sup>	0/3 (39.2 $\pm$ 0.1)	0/3	0	0	0/3 (<1) <sup>e</sup>

<sup>a</sup> Rectal temperatures higher than 39.5°C are considered pyrexia in pigs. Peak rectal temperatures are expressed as means  $\pm$  standard deviations (SD).

<sup>b</sup> The directly infected pigs were euthanized at 6 dpi and the in-contact pigs at 7 dpc (8 dpi). Percentages are based on the pulmonary consolidation area, and the values are expressed as mean percentages  $\pm$  SD.

<sup>c</sup> Microscopic lung lesions were assigned a score of 0 to 4. Scores are expressed as means  $\pm$  SD.

<sup>d</sup> Virus titers are expressed as mean log<sub>10</sub> TCID<sub>50</sub>/g  $\pm$  SD.

<sup>e</sup> Lower than the detection limit of 10 TCID<sub>50</sub>/g.

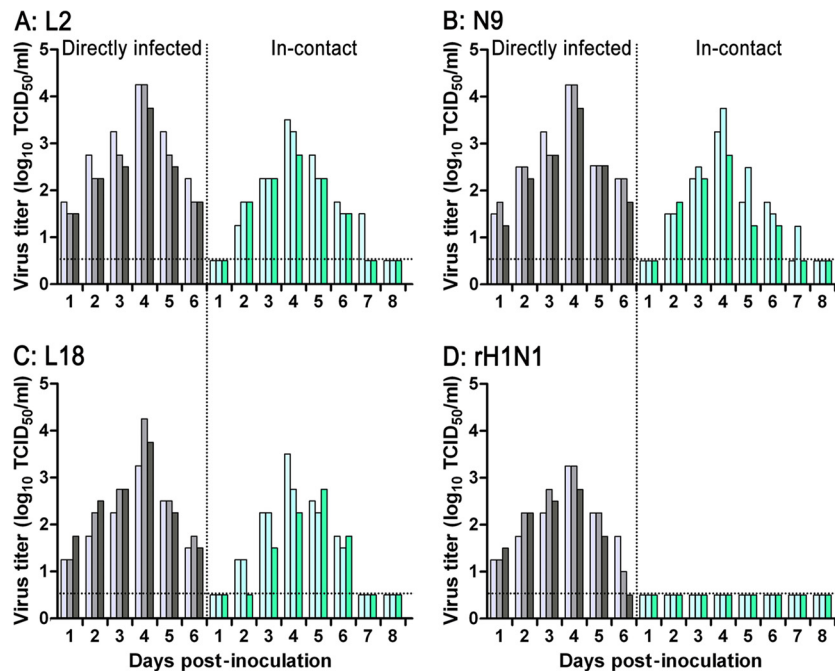


**FIG 8** In-contact transmission of viruses derived from P9 virus-derived L2, N9, and L18 viruses in pigs. Groups of three pigs (4 to 5 weeks old) were infected intranasally with  $10^6$  TCID<sub>50</sub> of L2 (A), N9 (B), L18 (C), and parental control rH1N1 (D) viruses. Three naive animals were introduced into each group 24 h later. Unlike parental rH1N1 virus, all three P9-derived viruses were efficiently transmitted to all in-contact pigs. Virus titers in nasal swabs were determined by TCID<sub>50</sub> assays on MDCK cells at the indicated dpi or dpc. The horizontal dashed line corresponds to the TCID<sub>50</sub> assay detection limit. Each bar represents the virus titer from an individual animal.

Among these six viruses, the PB1 A469T-only mutation infected one of three contact guinea pigs (Fig. 10A and E), and NS1 N205K and NEP T48N mutation infected two of three contact animals (Fig. 10D and F). However, no virus shedding was detected in any contact animals from the PA I129T and NA N329D groups (Fig. 10B and C). These results indicated that PB1 A469T, combined NS1 N205K and NEP T48N single-site mutations in the parental rH1N1 virus, conferred enhanced in-contact transmissibility in guinea pigs. Additionally, virus output from these transmissible rH1N1 mutants at 5.75 to 7.25 log<sub>10</sub> TCID<sub>50</sub>/ml (Fig. 9B to D and 10A and D to F) was significantly higher than that of the nontransmissible rH1N1 mutants at 4.25 to 5.75 log<sub>10</sub> TCID<sub>50</sub>/ml (Fig. 9A and 10B and C) ( $P < 0.05$ ), which suggested that the transmissibility of mutant PB1 A469T and combined mutant NS1 N205K and NEP T48N in guinea pigs also was related to enhanced virus replication. No obvious clinical signs were observed in any of the infected and uninfected guinea pigs during the observation period, and all animals with viral shedding also showed seroconversion (data not shown).

**Severe pathogenicity and respiratory droplet transmission of representative P9-derived viruses in ferrets.** Ferrets have been widely used as an experimental model to study human infection and transmission of influenza virus (13, 26). Three ferrets were infected intranasally with each virus (L2, N9, L18, and parental rH1N1 viruses) at a dose of  $10^6$  TCID<sub>50</sub>. Directly infected ferrets were individually caged and sited in close proximity to individually kept naive ferrets (5 cm away).

All ferrets directly infected with P9 virus-derived L2, N9, and L18 viruses developed severe clinical symptoms (pyrexia, lethargy, anorexia, sneezing, wheezing, and coughing) from 2 to 8 dpi, in-

cluding one death from L2 virus infection at 7 dpi (Table 3). However, all rH1N1 virus-infected ferrets developed only mild clinical signs of slight pyrexia, anorexia, and sneezing at 2 to 4 dpi (Table 3). At postmortem at 8 dpi, gross and histopathological lesions, including severe consolidation (>40%), hemorrhage, and edema, were evident in all ferrets infected with the three P9-derived viruses. In contrast, little or no lung consolidation (0% to 5%) was found in parental rH1N1 virus-infected ferrets (Fig. 11 and Table 3). These results demonstrate that the three P9-derived viruses (L2, N9, and L18) were much more pathogenic than the parental rH1N1 virus in ferrets.

To assess the transmissibility of the P9-derived viruses in ferrets, we compared virus titers in nasal washes from directly infected and proximally exposed ferrets. High levels of virus shedding were evident for all directly infected ferrets (>6.25 log<sub>10</sub> TCID<sub>50</sub>/ml at 2 to 4 dpi), which was about 10- to 100-fold greater than that of the corresponding rH1N1 virus group (Fig. 12). However, for proximally exposed ferrets, only the group associated with the L2 virus was found to shed virus continuously in all three exposed ferrets and at levels comparable to that of the directly infected ferrets (Fig. 12A). Notably, the high levels of L2 virus replication in directly infected and proximally exposed ferrets were highly similar to corresponding reported findings of H1N1/2009 viruses (27, 28). Additionally, all proximally exposed L2 ferrets showed severe clinical signs and pulmonary damage (Fig. 11 and Table 3). Taken together, these results demonstrate that the three representative P9-derived viruses (L2, N9, and L18) had acquired enhanced replication and pathogenicity in ferrets, and that L2 virus additionally was highly effective in airborne transmission in ferrets. The latter finding suggests that the HA mutations



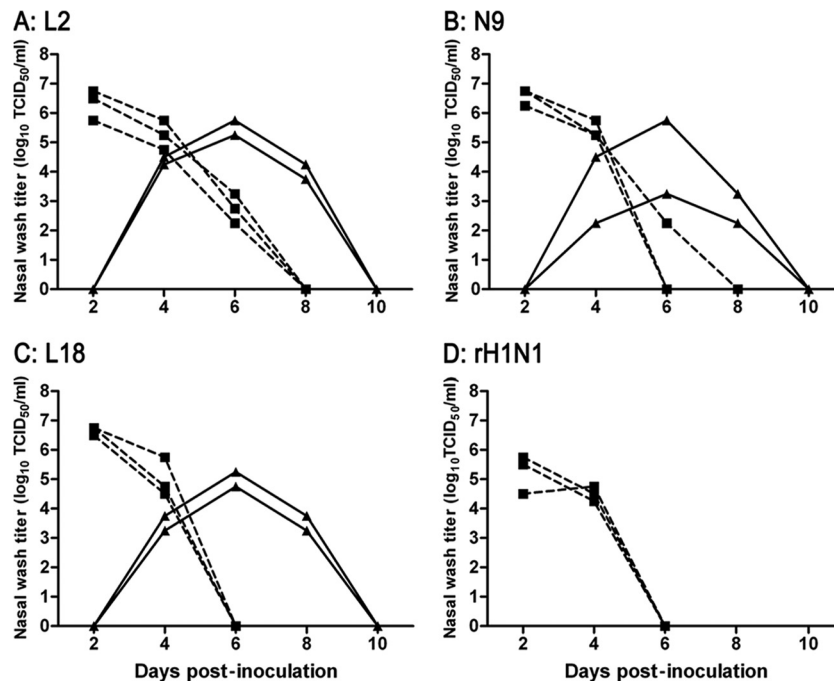


FIG 9 In-contact transmission of P9 virus-derived L2, N9, and L18 viruses in guinea pigs. Four groups of guinea pigs (three to a group) each were intranasally inoculated with  $10^6$  TCID<sub>50</sub> of L2 (A), N9 (B), L18 (C), or rH1N1 (D) virus. At 1 dpi, each directly infected animal (individually housed) was moved to another cage holding a naive guinea pig. Viral titers of daily nasal washes were determined by TCID<sub>50</sub> assays on MDCK cells from the directly infected (squares with dotted lines) and in-contact guinea pigs (triangles with solid lines) and are presented as a function of days postvirus inoculation. Two out of three in-contact guinea pigs for each P9-derived virus showed virus shedding. There was no detectable rH1N1 virus shedding from in-contact guinea pigs. The virus detection limit was 10 TCID<sub>50</sub>.

(D187E, K211E, and S289N) in the L12 virus contribute to its airborne transmission ability.

## DISCUSSION

The pandemic H1N1/2009 virus is thought to have been generated in swine and circulated in pig populations before its cross-species transmission to humans; however, despite considerable research, this has not been proven (2, 3, 6). Here, we serially passaged an engineered H1N1/2009-like precursor (rH1N1) virus in pigs to simulate a probable evolutionary emergence route of the H1N1/2009 virus. Dramatic changes in viral characteristics occurred after just nine serial passages, including enhanced replication and polymerase activity *in vitro*, increased pathogenicity in pigs and ferrets, and efficient in-contact transmission in pigs and guinea pigs. Furthermore, a P9-derived clone (L2 virus) even acquired highly efficient respiratory droplet transmissibility in ferrets, a property which was similar to that of the H1N1/2009 virus.

Adaptation is believed to be a driving force in evolution, whereby organisms, including viruses, are selected in nature because of increased fitness conferred by gene mutations (24). For IAVs, adaptive evolution does not act on a single virion but on quasispecies, which represent populations of diverse variants that are genetically similar and collectively contribute to the characteristics of the population (24, 29). Here, we used deep sequencing to examine the mutations and frequency of the viral quasispecies in the upper (nasal wash) and lower (BALF) respiratory tracts of the P9 virus-infected pigs. We found five consensus amino acid mutations in all of the quasispecies in both compartments, indicating

rapid mutational selection in limited serial passages. However, mutations in the HA gene exhibited marked differences between nasal wash and BALF, revealing evolutionary divergence of HA genes between upper and lower airways within an animal. The cause for this mutational divergence could be related to the virus itself, cell surface receptors, cell types, and antibody binding (30–32). Moreover, the frequencies of HA mutations varied in the upper and lower respiratory tracts. This finding was verified by sequencing single viral clones, which reflected complex combinations of dominant and/or sporadic mutations in HA proteins within each location of the airway (see Table S1 in the supplemental material). This phenomenon shares some similarities with the findings of Murcia et al. (33) with regard to the evolutionary dynamics of a Eurasian avian-like swine influenza virus along the natural transmission chain. They observed a highly dynamic mutational spectrum with both transient and fixed mutations in the HA gene derived from consecutive daily nasal virus populations. We speculate that there are two kinds of evolutionary processes at work in the convergent evolution of influenza virions, high-frequency mutagenesis and rapid allele fixation, and such an evolutionary scheme readily facilitates IAV infection and transmission in new host species.

Most reported triple-reassortant swine H1 viruses caused mild disease, were inefficiently transmitted through the air in ferrets (34, 35), and had restricted circulation in humans (36), even though they generally possess strong binding affinity for the  $\alpha 2,6$ -linked human-like receptor (37). Our previous (7) and present studies demonstrated that the parental rH1N1 virus had viral characteristics identical to those of these reported triple-reas-

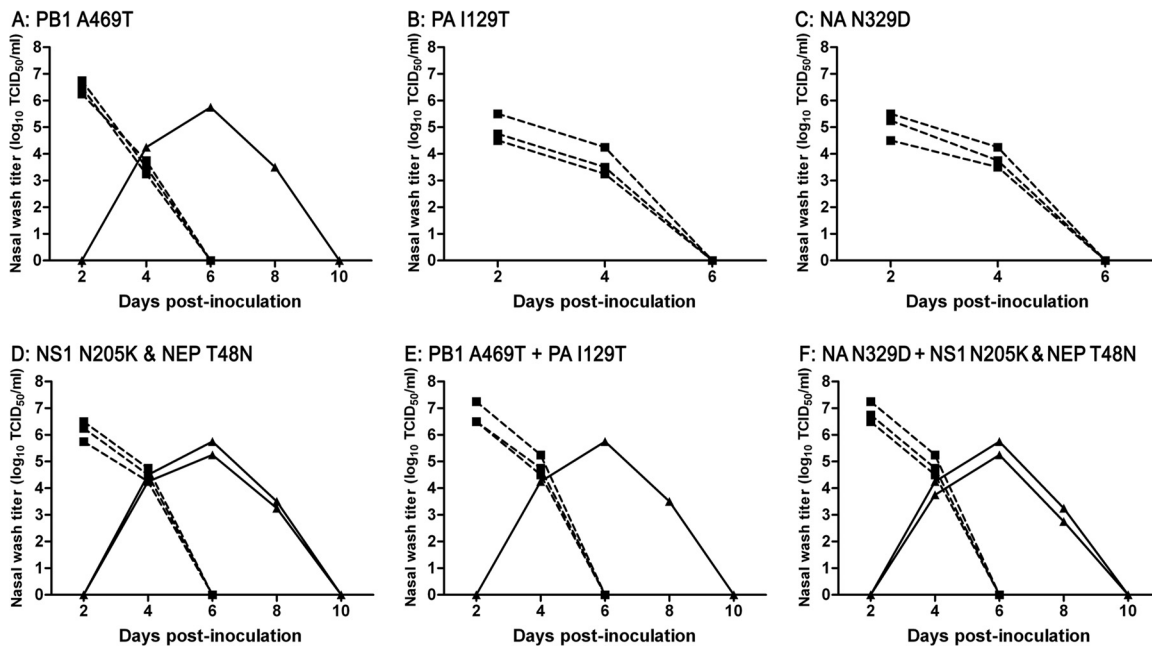


**FIG 10** In-contact transmission of mutant rH1N1 viruses in guinea pigs. Guinea pigs (in six groups of three) each were intranasally inoculated with  $10^6$  TCID<sub>50</sub> of PB1 A469T (A), PA I129T (B), NA N329D (C), the combined NS1 N205K and NEP T48N (NS1 N205K & NEP T48N) (D), the combined PB1 A469T and PA I129T (PB1 A469T + PA I129T) (E), or the combined NA N329D, NS1 N205K, and NEP T48N (NA N329D + NS1 N205K & NEP T48N) (F) virus. At 1 dpi, each directly infected animal (individually housed) was moved to another cage holding a naive guinea pig. Viral titers of daily nasal washes were determined by TCID<sub>50</sub> assays on MDCK cells from the directly infected (squares with dotted lines) and in-contact guinea pigs (triangles with solid lines) and are presented as a function of days postvirus inoculation. Infections with the PB1 A469T mutant and combined NS1 N205K and NEP T48N mutant viruses were transmissible to one and two in-contact guinea pigs, respectively. The virus detection limit was  $10$  TCID<sub>50</sub>.

sortant viruses. Crucially, we found that by passage nine in pigs, the replication and pathogenicity of three representative mutants (L2, N9, and L18) greatly exceeded those of the parental rH1N1 virus in both pigs and ferrets. More importantly, the three viruses had enhanced contact transmissibility in both pigs and guinea pigs. Their enhanced virulence and contact transmissibility were similar to that of the H1N1/2009 virus (38–40). Since the virulence and contact transmissibility were comparable between the L2, N9, and L18 viruses, these acquired traits were determined primarily by the five consensus mutations (PB1 A469T, PA I129T, NA N329D, NS1 N205K, and NEP T48N) found in all three virus species. Furthermore, guinea pig experiments demonstrated that the PB1 A469T mutation and the combined NS1 N205K and NEP T48N mutations in rH1N1 virus conferred in-contact transmissibility in guinea pigs.

Viral polymerase may be the driving component of early evolution of an IAV in a new host, and polymerase-enhancing mutations could contribute to the increased replication and virulence of IAVs (10, 25, 41). We observed significantly enhanced polymerase activity with the PB1 A469T mutation in the parental rH1N1 RNP complex. Residue position 469 locates to a site involved in RNA polymerase activity (42), and sequence analysis revealed that PB1 469T is conserved in pandemic H1N1/2009 isolates, which could be an important pathogenicity determinant of the pandemic H1N1/2009 virus. Our previous studies have demonstrated that the NS gene of H1N1/2009 origin is critical for contact transmission of the rH1N1 virus in guinea pigs (7). Zhang et al. have reported that the NS gene of H1N1/2009 virus can confer H5N1 virus transmission by respiratory droplet between guinea pigs (43). For the combined NS1 N205K and NEP T48N mutant virus,

we could not readily verify which one of the two proteins plays a major role in guinea pig transmissibility, as both changes are the result of a single-nucleotide change. We do know that NS1 protein of IAV is a multifunctional virulence factor that inhibits host cell pre-mRNA processing and counteracts host cell antiviral responses. Residue 205 is located in the C terminus (residues 201 to 230) of NS1, and this tail has been implicated in the interaction of NS1 with cleavage and polyadenylation specificity factor (CPSF), poly(A)-binding protein II (PAB II), and host importins (44–46). It is likely that the NS1 N205K mutation plays a role in the pathogenesis of IAV by influencing these interactions. NEP, formerly called NS2, has been demonstrated to mediate the export of viral RNP complexes from the nucleus (47) and to act as a quantitative switch from viral transcription during early viral replication to favor late-stage production of genomic vRNPs (48). Additionally, NEP also has been implicated in recruiting a cellular ATPase to the cell membrane to aid the efficient release of budding virions (49, 50). Accordingly, NEP is proposed to play multiple biologically important roles during the life cycle of IAVs; thus, NEP T48N mutation could alter the replication and transmission characteristics of the rH1N1 virus.

A hallmark of the pandemic H1N1/2009 virus is its efficient transmission in humans (51, 52). In the present study, we found that the P9-derived L2 virus was efficiently transmitted through the air in ferrets (a recognized model of human influenza virus infection), as observed with the pandemic H1N1/2009 virus (27, 28). This suggests that the five consensus mutations are responsible for the enhanced virulence, and that the HA mutations (D187E, K211E, and S289N) in the L2 virus are linked to effective airborne transmission in ferrets. The receptor binding specificity

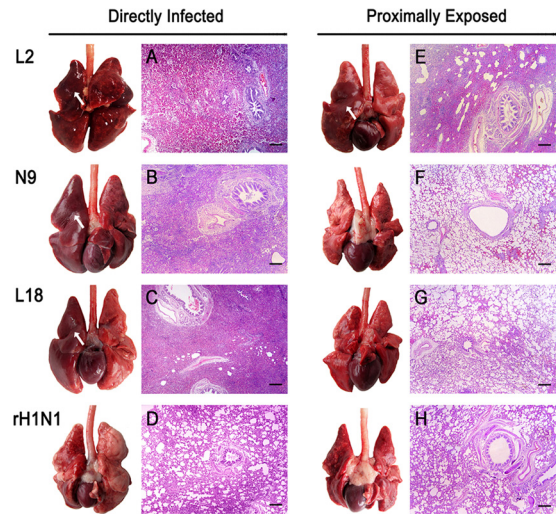


**FIG 11** Gross pathology and histopathology of lungs from ferrets infected with three representative P9-derived viruses (L2, N9, and L18). Lungs were isolated from ferrets directly infected with L2, N9, L18, and rH1N1 viruses at 8 dpi or from ferrets proximally exposed for 9 days (10 dpi) to infected ones. (A to C and E) Lungs from pigs directly infected L2, N9, and L18 viruses, along with lungs of L2 virus-exposed pigs, showed extensive edema, consolidation (white arrows), severe interstitial pneumonia with infiltration of erythrocytes, and inflammatory cells in the alveolar space. (D) The directly infected rH1N1 lung showed mild edema, emphysema, and mild bronchopneumonia. (F to H) Lungs of ferrets proximally exposed to ferrets directly infected with N9, L18, and rH1N1 viruses showed no obvious gross lesions or pathological damage. Images shown are representative of three ferrets from three independent experiments. Scale bar, 200  $\mu$ m.

of HA has been implicated in interspecies transmission of IAVs (53, 54). Binding to the  $\alpha$ 2,6-linked sialic acid receptor is thought to be a critical prerequisite for IAVs to cross the species barrier and to adapt to the human host (55, 56). We also determined the receptor-binding properties of the three P9-derived viral clones using direct glycan receptor-binding assays and found that all three P9-derived viruses retained the  $\alpha$ 2,6-linked receptor binding specificity of the parental rH1N1 virus (data not shown). Hence,  $\alpha$ 2,6-linked receptor binding specificity alone could not mediate airborne transmission. We surmise that the three mutations in HA of L2 virus play a role in its function after cell entry, such as in its acid stability, which is associated with the conformational change of HA and fusion of the viral and endosomal membranes in the release of the virus genome into the cytoplasm (57). Further study will be needed to examine the critical genetic changes in airborne L2 virus, especially those in the HA protein.

Finally, the identified mutations (except for the PB1 A469T mutation), linked to enhanced pathogenicity and transmissibility (in-contact and aerosol spread), which arose from serial passage in pigs, were not found in the H1N1/2009 virus. These mismatches are not entirely surprising, as there are about 180 amino acid differences between the parental rH1N1 virus and the early pandemic H1N1/2009 virus. Such differences suggest that gain in pathogenicity and transmissibility can be achieved through different combinations of amino acid changes in the virus. We demonstrated that pigs can independently facilitate such combinatorial changes in the genesis of a potential human pandemic strain for which all gene segments are of swine origin. Therefore, it would

**TABLE 3** Clinical symptoms, pathological changes, and viral shedding in ferrets

Infection characteristics in:													
Directly infected ferrets							Proximally exposed ferrets						
Virus	Pyrexia <sup>a</sup> (no. positive/ total no.)	Weight loss <sup>b</sup> (no. positive/ total no.) (%)	Sneezing/ coughing/ total no.)	Lethality (no. positive/ total no.)	Pulmonary consolidation <sup>c</sup> (no. positive/ total no.) (%)	Microscopic lung lesion score <sup>d</sup>	Virus shedding <sup>e</sup> (no. positive/ total no.)	Pyrexia <sup>a</sup> (no. positive/ total no.)	Weight loss <sup>b</sup> (no. positive/ total no.) (%)	Sneezing/ coughing/ total no.)	Pulmonary consolidation <sup>c</sup> (no. positive/ total no.) (%)	Microscopic lung lesion score <sup>d</sup>	Virus shedding <sup>e</sup> (no. positive/ total no.)
L2	3/3 (40.2 $\pm$ 0.2)	3/3 (19.5 $\pm$ 3.6)	3/3	1/3	3/3 (90, 60, 55)	3.6 $\pm$ 0.3	3/3	3/3 (40.1 $\pm$ 0.2)	3/3 (11.0 $\pm$ 1.8)	3/3	3/3 (40, 25, 20)	2.6 $\pm$ 0.3	3/3
N9	3/3 (40.0 $\pm$ 0.1)	3/3 (15.3 $\pm$ 4.2)	3/3	0/3	3/3 (60, 50, 40)	3.3 $\pm$ 0.3	3/3	3/3 (38.0 $\pm$ 0.3)	0/3	0/3	0/3	0.3 $\pm$ 0.1 <sup>f</sup>	0/3
L18	3/3 (39.9 $\pm$ 0.1)	3/3 (16.1 $\pm$ 2.8)	3/3	0/3	3/3 (60, 55, 50)	3.3 $\pm$ 0.3	3/3	3/3 (38.1 $\pm$ 0.2)	0/3	0/3	0/3	0.3 $\pm$ 0.1	0/3
rH1N1	1/3 (38.0 $\pm$ 0.1)	2/3 (5.6 $\pm$ 1.7)	1/3	0/3	2/3 (5, 5, 0)	0.8 $\pm$ 0.1	3/3	0/3 (37.9 $\pm$ 0.3)	0/3	0/3	0/3	0.3 $\pm$ 0.1	0/3

<sup>a</sup> Rectal temperatures higher than 39°C are considered pyrexia in ferrets. Peak rectal temperatures are expressed in parentheses as means  $\pm$  SD.

<sup>b</sup> Weight loss is expressed as mean maximum percentages  $\pm$  SD during the observation time.

<sup>c</sup> The directly infected ferrets were euthanized at 8 dpi and the proximally exposed ferret at 9 dpi (10 dpi). Percentages are based on the pulmonary consolidation area, and the value for each animal is listed separately.

<sup>d</sup> Microscopic lung lesions were assigned a score of 0 to 4. Scores are expressed as means  $\pm$  SD.

<sup>e</sup> Virus titers in nasal washes are shown in Fig. 12.

<sup>f</sup> The lung had incidental non-influenza virus-associated lung lesions caused by continual sampling.



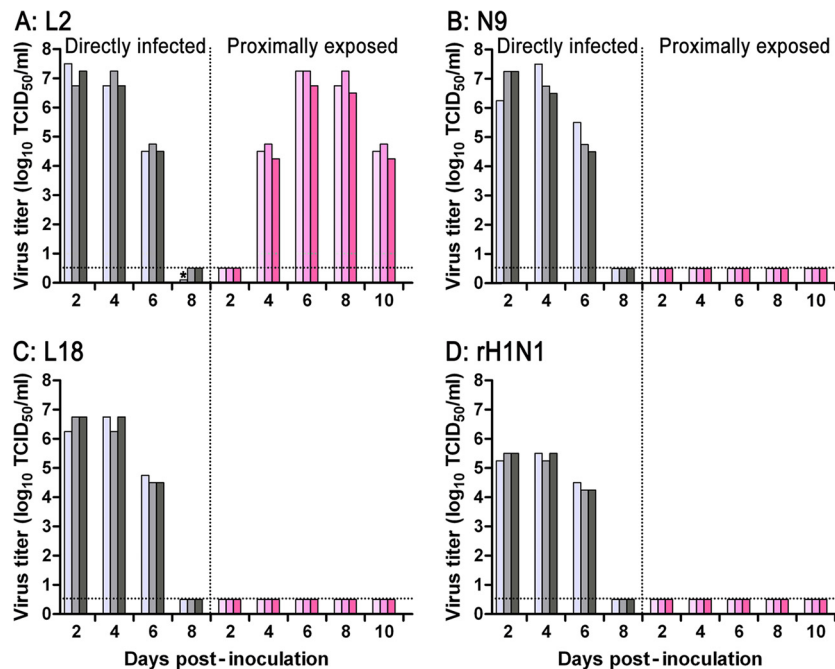


**FIG 12** Efficient respiratory droplet transmission of P9 virus-derived L2 virus in ferrets. Three ferrets were intranasally inoculated with  $10^6$  TCID<sub>50</sub> of L2 (A), N9 (B), L18 (C), or parental rH1N1 (D) virus. Each infected animal was individually housed next to a naive ferret in an adjacent cage (5 cm away). Virus titers of nasal washes were determined by TCID<sub>50</sub> assays on MDCK cells and plotted as directly infected and proximally exposed groups of animals against the number of days after virus inoculation. The horizontal dashed line represents the detection limit of the TCID<sub>50</sub> assay. Each bar represents the virus titer from an individual animal. The asterisk indicates a ferret that died at 7 dpi.

have been highly feasible for the generation of the emergent pandemic virus to have begun in swine, although we are still unable to determine whether other host species were involved in the evolution of pandemic H1N1/2009 virus prior to its jump into humans. Altogether, our findings emphasize the importance of continued monitoring of influenza viruses in pigs.

## ACKNOWLEDGMENTS

We thank Lu Qi, Meng Yu, Guanlong Xu, Yandi Wei, Linqing Liu, Huijie Gao, Xiaolin Zhu, and Seng Lai Giea for excellent technical assistance.

This work was supported by the National Science Fund for Distinguished Young Scholars (31025029), the National Basic Research Program (973 Program; 2011CB504702), the National Natural Science Foundation of China (31172323 and 31172324), and the Biotechnology and Biological Sciences Research Council (UK) China Partnering Award.

## REFERENCES

- Trifonov V, Khiabani H, Rabadan R. 2009. Geographic dependence, surveillance, and origins of the 2009 influenza A (H1N1) virus. *N. Engl. J. Med.* 361:115–119. <http://dx.doi.org/10.1056/NEJMp0904572>.
- Smith GJ, Vijaykrishna D, Bahl J, Lycett SJ, Worobey M, Pybus OG, Ma SK, Cheung CL, Raghwani J, Bhatt S. 2009. Origins and evolutionary genomics of the 2009 swine-origin H1N1 influenza A epidemic. *Nature* 459:1122–1125. <http://dx.doi.org/10.1038/nature08182>.
- Garten RJ, Davis CT, Russell CA, Shu B, Lindstrom S, Balish A, Sessions WM, Xu X, Skepner E, Deyde V. 2009. Antigenic and genetic characteristics of swine-origin 2009 A (H1N1) influenza viruses circulating in humans. *Science* 325:197–201. <http://dx.doi.org/10.1126/science.1176225>.
- Xu R, Ekiert DC, Krause JC, Hai R, Crowe JE, Wilson IA. 2010. Structural basis of preexisting immunity to the 2009 H1N1 pandemic influenza virus. *Science* 328:357–360. <http://dx.doi.org/10.1126/science.1186430>.
- Manicassamy B, Medina RA, Hai R, Tsibane T, Stertz S, Nistal-Villán E, Palese P, Basler CF, García-Sastre A. 2010. Protection of mice against lethal challenge with 2009 H1N1 influenza A virus by 1918-like and classical swine H1N1 based vaccines. *PLoS Pathog.* 6:e1000745. <http://dx.doi.org/10.1371/journal.ppat.1000745>.
- Vijaykrishna D, Smith GJ, Pybus OG, Zhu H, Bhatt S, Poon LL, Riley S, Bahl J, Ma SK, Cheung CL. 2011. Long-term evolution and transmission dynamics of swine influenza A virus. *Nature* 473:519–522. <http://dx.doi.org/10.1038/nature10004>.
- Zhao X, Sun Y, Pu J, Fan L, Shi W, Hu Y, Yang J, Xu Q, Wang J, Hou D. 2011. Characterization of an artificial swine-origin influenza virus with the same gene combination as H1N1/2009 virus: a genesis clue of pandemic strain. *PLoS One* 6:e22091. <http://dx.doi.org/10.1371/journal.pone.0022091>.
- Bouvier NM, Lowen AC. 2010. Animal models for influenza virus pathogenesis and transmission. *Viruses* 2:1530–1563. <http://dx.doi.org/10.3390/v20801530>.
- Medina RA, García-Sastre A. 2011. Influenza A viruses: new research developments. *Nat. Rev. Microbiol.* 9:590–603. <http://dx.doi.org/10.1038/nrmicro2613>.
- Gabriel G, Dauber B, Wolff T, Planz O, Klenk H-D, Stech J. 2005. The viral polymerase mediates adaptation of an avian influenza virus to a mammalian host. *Proc. Natl. Acad. Sci. U. S. A.* 102:18590–18595. <http://dx.doi.org/10.1073/pnas.0507415102>.
- Ping J, Dankar SK, Forbes NE, Keleta L, Zhou Y, Tyler S, Brown EG. 2010. PB2 and hemagglutinin mutations are major determinants of host range and virulence in mouse-adapted influenza A virus. *J. Virol.* 84:10606–10618. <http://dx.doi.org/10.1128/JVI.01187-10>.
- Lowen AC, Mubareka S, Tumpey TM, García-Sastre A, Palese P. 2006. The guinea pig as a transmission model for human influenza viruses. *Proc. Natl. Acad. Sci. U. S. A.* 103:9988–9992. <http://dx.doi.org/10.1073/pnas.0604157103>.
- Maher JA, DeStefano J. 2004. The ferret: an animal model to study influenza virus. *Lab Anim.* 33:50–53. <http://dx.doi.org/10.1038/labani004-50>.
- Chou Y-Y, Albrecht RA, Pica N, Lowen AC, Richt JA, García-Sastre A, Palese P, Hai R. 2011. The M segment of the 2009 new pandemic H1N1 influenza virus is critical for its high transmission efficiency in the guinea pig model. *J. Virol.* 85:11235–11241. <http://dx.doi.org/10.1128/JVI.05794-11>.

15. Herfst S, Schrauwen EJ, Linster M, Chutinimitkul S, de Wit E, Munster VJ, Sorrell EM, Bestebroer TM, Burke DF, Smith DJ. 2012. Airborne transmission of influenza A/H5N1 virus between ferrets. *Science* 336: 1534–1541. <http://dx.doi.org/10.1126/science.1213362>.
16. Imai M, Watanabe T, Hatta M, Das SC, Ozawa M, Shinya K, Zhong G, Hanson A, Katsura H, Watanabe S. 2012. Experimental adaptation of an influenza H5 HA confers respiratory droplet transmission to a reassortant H5 HA/H1N1 virus in ferrets. *Nature* 486:420–428.
17. Neumann G, Noda T, Kawaoka Y. 2009. Emergence and pandemic potential of swine-origin H1N1 influenza virus. *Nature* 459:931–939. <http://dx.doi.org/10.1038/nature08157>.
18. Pensaert M, Ottis K, Vandeputte J, Kaplan MM, Bachmann P. 1981. Evidence for the natural transmission of influenza A virus from wild ducks to swine and its potential importance for man. *Bull. World Health Organ.* 59:75–78.
19. Kida H, Ito T, Yasuda J, Shimizu Y, Itakura C, Shortridge KF, Kawaoka Y, Webster RG. 1994. Potential for transmission of avian influenza viruses to pigs. *J. Gen. Virol.* 75:2183–2188. <http://dx.doi.org/10.1099/0022-1317-75-9-2183>.
20. Castrucci MR, Donatelli I, Sidoli L, Barigazzi G, Kawaoka Y, Webster RG. 1993. Genetic reassortment between avian and human influenza A viruses in Italian pigs. *Virology* 193:503–506. <http://dx.doi.org/10.1006/viro.1993.1155>.
21. Reed LJ, Muench H. 1938. A simple method of estimating fifty per cent endpoints. *Am. J. Epidemiol.* 27:493–497.
22. Masic A, Booth JS, Mutwiri GK, Babiuk LA, Zhou Y. 2009. Elastase-dependent live attenuated swine influenza A viruses are immunogenic and confer protection against swine influenza A virus infection in pigs. *J. Virol.* 83:10198–10210. <http://dx.doi.org/10.1128/JVI.00926-09>.
23. Nowak MA. 1992. What is a quasispecies? *Trends Ecol. Evol.* 7:118–121. [http://dx.doi.org/10.1016/0169-5347\(92\)90145-2](http://dx.doi.org/10.1016/0169-5347(92)90145-2).
24. Domingo E, Holland J. 1997. RNA virus mutations and fitness for survival. *Annu. Rev. Microbiol.* 51:151–178. <http://dx.doi.org/10.1146/annurev.micro.51.1.151>.
25. Mehle A, Doudna JA. 2009. Adaptive strategies of the influenza virus polymerase for replication in humans. *Proc. Natl. Acad. Sci. U. S. A.* 106: 21312–21316. <http://dx.doi.org/10.1073/pnas.0911915106>.
26. Sweet C, Hayden FG, Jakeman KJ, Grambas S, Hay AJ. 1991. Virulence of rimantadine-resistant human influenza A (H3N2) viruses in ferrets. *J. Infect. Dis.* 164:969–972. <http://dx.doi.org/10.1093/infdis/164.5.969>.
27. Maines TR, Jayaraman A, Belser JA, Wadford DA, Pappas C, Zeng H, Gustin KM, Pearce MB, Viswanathan K, Shriver ZH. 2009. Transmission and pathogenesis of swine-origin 2009 A (H1N1) influenza viruses in ferrets and mice. *Science* 325:484–487. <http://dx.doi.org/10.1126/science.1177238>.
28. Munster VJ, de Wit E, van den Brand JM, Herfst S, Schrauwen EJ, Bestebroer TM, van de Vijver D, Boucher CA, Koopmans M, Rimmelzwaan GF. 2009. Pathogenesis and transmission of swine-origin 2009 A (H1N1) influenza virus in ferrets. *Science* 325:481–483. <http://dx.doi.org/10.1126/science.1177127>.
29. Lauring AS, Andino R. 2010. Quasispecies theory and the behavior of RNA viruses. *PLoS Pathog.* 6:e1001005. <http://dx.doi.org/10.1371/journal.ppat.1001005>.
30. Liu Y, Childs RA, Matrosovich T, Wharton S, Palma AS, Chai W, Daniels R, Gregory V, Uhlenhorff J, Kiso M. 2010. Altered receptor specificity and cell tropism of D222G hemagglutinin mutants isolated from fatal cases of pandemic A (H1N1) 2009 influenza virus. *J. Virol.* 84:12069–12074. <http://dx.doi.org/10.1128/JVI.01639-10>.
31. Matrosovich MN, Matrosovich TY, Gray T, Roberts NA, Klenk H-D. 2004. Human and avian influenza viruses target different cell types in cultures of human airway epithelium. *Proc. Natl. Acad. Sci. U. S. A.* 101: 4620–4624. <http://dx.doi.org/10.1073/pnas.0308001101>.
32. Skehel JJ, Wiley DC. 2000. Receptor binding and membrane fusion in virus entry: the influenza hemagglutinin. *Annu. Rev. Biochem.* 69:531–569. <http://dx.doi.org/10.1146/annurev.biochem.69.1.531>.
33. Murcia PR, Hughes J, Battista P, Lloyd L, Baillie GJ, Ramirez-Gonzalez RH, Ormond D, Oliver K, Elton D, Mumford JA. 2012. Evolution of an Eurasian avian-like influenza virus in naive and vaccinated pigs. *PLoS Pathog.* 8:e1002730. <http://dx.doi.org/10.1371/journal.ppat.1002730>.
34. Belser JA, Gustin KM, Maines TR, Blau DM, Zaki SR, Katz JM, Tumpey TM. 2011. Pathogenesis and transmission of triple-reassortant swine H1N1 influenza viruses isolated before the 2009 H1N1 pandemic. *J. Virol.* 85:1563–1572. <http://dx.doi.org/10.1128/JVI.02231-10>.
35. Pascua PNQ, Song M-S, Lee JH, Baek YH, Kwon H-I, Park S-J, Choi EH, Lim G-J, Lee O-J, Kim S-W. 2012. Virulence and transmissibility of H1N2 influenza virus in ferrets imply the continuing threat of triple-reassortant swine viruses. *Proc. Natl. Acad. Sci. U. S. A.* 109:15900–15905. <http://dx.doi.org/10.1073/pnas.1205576109>.
36. Shinde V, Bridges CB, Uyeki TM, Shu B, Balish A, Xu X, Lindstrom S, Gubareva LV, Deyde V, Garten RJ. 2009. Triple-reassortant swine influenza A (H1) in humans in the United States, 2005–2009. *N. Engl. J. Med.* 360:2616–2625. <http://dx.doi.org/10.1056/NEJMoa0903812>.
37. Gambaryan AS, Karasin AI, Tuzikov AB, Chinarev AA, Pazynina GV, Bovin NV, Matrosovich MN, Olsen CW, Klimov AI. 2005. Receptor-binding properties of swine influenza viruses isolated and propagated in MDCK cells. *Virus Res.* 114:15–22. <http://dx.doi.org/10.1016/j.virusres.2005.05.005>.
38. Chou YY, Albrecht RA, Pica N, Lowen AC, Richt JA, Garcia-Sastre A, Palese P, Hai R. 2011. The M segment of the 2009 new pandemic H1N1 influenza virus is critical for its high transmission efficiency in the guinea pig model. *J. Virol.* 85:11235–11241. <http://dx.doi.org/10.1128/JVI.05794-11>.
39. Brookes SM, Nunez A, Choudhury B, Matrosovich M, Essen SC, Clifford D, Slomka MJ, Kuntz-Simon G, Garcon F, Nash B, Hanna A, Heegaard PM, Queguiner S, Chiapponi C, Bublot M, Garcia JM, Gardner R, Foni E, Loeffen W, Larsen L, Van Reeth K, Banks J, Irvine RM, Brown IH. 2010. Replication, pathogenesis and transmission of pandemic (H1N1) 2009 virus in non-immune pigs. *PLoS One* 5:e9068. <http://dx.doi.org/10.1371/journal.pone.0009068>.
40. Ma W, Liu Q, Bawa B, Qiao C, Qi W, Shen H, Chen Y, Ma J, Li X, Webby RJ, Garcia-Sastre A, Richt JA. 2012. The neuraminidase and matrix genes of the 2009 pandemic influenza H1N1 virus cooperate functionally to facilitate efficient replication and transmissibility in pigs. *J. Gen. Virol.* 93:1261–1268. <http://dx.doi.org/10.1099/vir.0.040535-0>.
41. Salomon R, Franks J, Govorkova EA, Ilyushina NA, Yen H-L, Hulse-Post DJ, Humbert J, Trichet M, Rehg JE, Webby RJ. 2006. The polymerase complex genes contribute to the high virulence of the human H5N1 influenza virus isolate A/Vietnam/1203/04. *J. Exp. Med.* 203:689–697. <http://dx.doi.org/10.1084/jem.20051938>.
42. Ping J, Keleta L, Forbes NE, Dankar S, Stecho W, Tyler S, Zhou Y, Babiuk L, Weingartl H, Halpin RA. 2011. Genomic and protein structural maps of adaptive evolution of human influenza A virus to increased virulence in the mouse. *PLoS One* 6:e21740. <http://dx.doi.org/10.1371/journal.pone.0021740>.
43. Zhang Y, Zhang Q, Kong H, Jiang Y, Gao Y, Deng G, Shi J, Tian G, Liu L, Liu J. 2013. H5N1 hybrid viruses bearing 2009/H1N1 virus genes transmit in guinea pigs by respiratory droplet. *Science* 340:1459–1463. <http://dx.doi.org/10.1126/science.1229455>.
44. Li Y, Chen ZY, Wang W, Baker CC, Krug RM. 2001. The 3'-end-processing factor CPSF is required for the splicing of single-intron pre-mRNAs in vivo. *RNA* 7:920–931. <http://dx.doi.org/10.1017/S1355838201010226>.
45. Melen K, Kinnunen L, Fagerlund R, Ikonen N, Twu KY, Krug RM, Julkunen I. 2007. Nuclear and nucleolar targeting of influenza A virus NS1 protein: striking differences between different virus subtypes. *J. Virol.* 81:5995–6006. <http://dx.doi.org/10.1128/JVI.01714-06>.
46. Chen Z, Li Y, Krug RM. 1999. Influenza A virus NS1 protein targets poly(A)-binding protein II of the cellular 3'-end processing machinery. *EMBO J.* 18:2273–2283. <http://dx.doi.org/10.1093/emboj/18.8.2273>.
47. Neumann G, Hughes MT, Kawaoka Y. 2000. Influenza A virus NS2 protein mediates vRNP nuclear export through NES-independent interaction with hCRM1. *EMBO J.* 19:6751–6758. <http://dx.doi.org/10.1093/emboj/19.24.6751>.
48. Robb NC, Smith M, Vreede FT, Fodor E. 2009. NS2/NEP protein regulates transcription and replication of the influenza virus RNA genome. *J. Gen. Virol.* 90:1398–1407. <http://dx.doi.org/10.1099/vir.0.009639-0>.
49. Gorai T, Goto H, Noda T, Watanabe T, Kozuka-Hata H, Oyama M, Takano R, Neumann G, Watanabe S, Kawaoka Y. 2012. F1Fo-ATPase, F-type proton-translocating ATPase, at the plasma membrane is critical for efficient influenza virus budding. *Proc. Natl. Acad. Sci. U. S. A.* 109: 4615–4620. <http://dx.doi.org/10.1073/pnas.1114728109>.
50. Manz B, Brunotte L, Reuther P, Schwemmler M. 2012. Adaptive mutations in NEP compensate for defective H5N1 RNA replication in cultured human cells. *Nat. Commun.* 3:802. <http://dx.doi.org/10.1038/ncomms1804>.
51. Novel Swine-Origin Influenza A (H1N1) Virus Investigation Team, Dawood FS, Jain S, Finelli L, Shaw MW, Lindstrom S, Garten RJ, Gubareva LV, Xu X, Bridges CB, Uyeki TM. 2009. Emergence of a novel

- swine-origin influenza A (H1N1) virus in humans. *N. Engl. J. Med.* 360: 2605–2615. <http://dx.doi.org/10.1056/NEJMoa0903810>.
52. Zarocostas J. 2009. World Health Organization declares A (H1N1) influenza pandemic. *BMJ* 338:b2425. <http://dx.doi.org/10.1136/bmj.b2425>.
53. Tumpey TM, Maines TR, Van Hoeven N, Glaser L, Solórzano A, Pappas C, Cox NJ, Swayne DE, Palese P, Katz JM. 2007. A two-amino acid change in the hemagglutinin of the 1918 influenza virus abolishes transmission. *Science* 315:655–659. <http://dx.doi.org/10.1126/science.1136212>.
54. Imai M, Kawaoka Y. 2012. The role of receptor binding specificity in interspecies transmission of influenza viruses. *Curr. Opin. Virol.* 2:160–167. <http://dx.doi.org/10.1016/j.coviro.2012.03.003>.
55. Suzuki Y, Ito T, Suzuki T, Holland RE, Chambers TM, Kiso M, Ishida H, Kawaoka Y. 2000. Sialic acid species as a determinant of the host range of influenza A viruses. *J. Virol.* 74:11825–11831. <http://dx.doi.org/10.1128/JVI.74.24.11825-11831.2000>.
56. Yamada S, Suzuki Y, Suzuki T, Le MQ, Nidom CA, Sakai-Tagawa Y, Muramoto Y, Ito M, Kiso M, Horimoto T. 2006. Haemagglutinin mutations responsible for the binding of H5N1 influenza A viruses to human-type receptors. *Nature* 444:378–382. <http://dx.doi.org/10.1038/nature05264>.
57. Thoennes S, Li ZN, Lee BJ, Langley WA, Skehel JJ, Russell RJ, Steinhauer DA. 2008. Analysis of residues near the fusion peptide in the influenza hemagglutinin structure for roles in triggering membrane fusion. *Virology* 370:403–414. <http://dx.doi.org/10.1016/j.virol.2007.08.035>.